Method to measure the quality of a neuron model compared to recorded data

Oscar Flodin

LUND UNIVERSITY

Department of Automatic Control

MSc Thesis
ISSN 0280-5316
TFRT--6005

Department of Automatic Control
Lund University
Box 118
SE-221 00 LUND
Sweden

Printed in Sweden by Tryckeriet i E-huset
Lund 2016

Abstract

In this thesis, a method for evaluating the accuracy of mathematical neuron models is developed, with the objective to both improve the quality and the speed of parameter optimization. To evaluate the method, we used a conductance based model of the cuneate nucleus. The model behavior was evaluated against neurons recorded in vivo. A big challenge when modeling neurons is the timing of the action potentials, since the initiation is stochastic. Therefore, the model artificially inserts the spikes at the recorded spike times. The accuracy of the model is evaluated as its capacity to capture the time evolution of the membrane potential both following and preceding the spikes. The evaluation method uses the L2-norm when comparing a few important time windows of the recording and the model. The method was used to optimize the parameters of the model. Sensitivity analysis is used to learn which model parameters affect the model accuracy the most. The results from the optimization showed that the developed method well describes the quality of the neuron model for different parameters. This tool will make it easier to build models that capture the responsive properties of the membrane potential in neuronal *in vivo* recordings.

Acknowledgements

First and foremost, praise and thanks goes to my savior Jesus Christ for brilliantly creating this complex world and by his grace giving me the opportunity to study it.

I would like to give a special thanks to my supervisor Dr. Anton Spanne, with whom I have discussed many challenges that I have faced while working on this thesis.

I would also like to thank my supervisor Dr. Kristian Soltesz for a thorough proof-reading of the report.

Finally I would like to thank my supervisors Carolina Lidström and Dr. Henrik Jörntell for supporting me while working on this thesis. I would also like to acknowledge the student Johanna Norrlid, who has given me many laughs and an insight of the medical world.

Nomenclature

CN	cuneate nuclues	page 13
LVA	low voltage activated	page 16
HVA	high voltage activated	page 17
SA	sensitivity analysis	page 19
OAT	one at a time	page 19
GSA	global sensitivity analysis	page 19
EE	elementary effects	page 20
RMS	root mean square	page 23

Contents

1

Introduction

1.1 Background

The brain consists of billions of nerve cells, or neurons, that communicate with each other. A first step of understanding the brain is to understand how neurons work. Many modeling studies are carried out every year to understand how the different parts of the brain work, for a few examples see [LeMasson et al., 1993; Liu et al., 1998; Siegel et al., 1994; Taylor et al., 2009]. When studying the brain, relevant *in vivo* data are not always accessible. When experimental data are accessible, good methods to evaluate neuron models of the data might be lacking. Thus, a new method for measuring the quality of a neuron model would be a useful contribution to the science community. It is especially relevant to study the cuneate nucleus because its spontaneous activity is known and it is a limited system that only processes sensory information from the forelimbs [Jörntell et al., 2014]. Thus, it is interesting to understand how this network is set up and to investigate this. To this end, a detailed model of these neurons is necessary.

1.2 Statement of the problem

The main purpose of this thesis is to propose an evaluation method or goodness measure that define how well a neuron model mimics neuronal recordings. The availability of such a measure would enable us to conduct parameter sensitivity analysis and optimization. Several studies show that there are differences between neuron recordings and mathematical models such as the conductance based Hodgkin-Huxley model [Hodgkin and Huxley, 1952; Naundorf et al., 2006], but there is no consensus on how to quantify such discrepancies.

1.3 Method overview

This project will be based on intracellular *in vivo* recordings from a part of the brain called the cuneate nucleus [Jörntell et al., 2014]. One of the reasons that record-

ings from the neurons in the cuneate nucleus are being used is that it is relatively easy to control what information the cells receive when the electrical potential over the cell membrane is recorded since they mainly receive sensory information from the skin. The fact that it is relatively easy to control what information the cells receive is expected to make it easier to measure how well the model captures what is happening in the real neuron. The work will be done based on a model of Hodgkin-Huxley formalism [Hodgkin and Huxley, 1952], where the action potentials (also called spikes) will be generated artificially. A model for the projection neurons in the cuneate nucleus has been developed [Spanne, 2011]. The projection neurons transmit information from the nucleus to other parts of the brain. The model has a calcium dynamic that resembles what happens in the real cell. This model will be modified and used in this project. The evaluation method will be developed by first comparing the visual similarity of the model and the intracellular recordings and then finding a way to numerically quantify the differences between the model and the data. When developing the evaluation method, already existing methods need to be investigated. Similar problems have been examined by [Lepora et al., 2012] and [Brookings et al., 2014]. The next step is to use this method to optimize the parameters of the model.

Another important step in the process of parameter optimization is sensitivity analysis which will be carried out to investigate which parameters contributes the most to the variance of the quality of the model. Some parameters can possibly be excluded from the optimization if it turns out that they can be varied a lot without affecting the output of the model.

All experimental data used in this thesis are *in vivo* recordings from the cat brain, provided by Henrik Jörntell at the Department of Experimental Medical Sciences, Section for Neurophysiology, Lund University

2

Theory

2.1 The neuron model

The membrane potential is created and sustained by the outflow and inflow of electrically charged ions through the ion channels in the cell membrane. Neurons communicate by action potentials (also called spikes) that propagate through a network of dendrites and axons. These action potentials are all-or-none events that could be compared to a Dirac pulse in a mathematical context or in a computer setting a binary signal. In the time domain, the duration of an action potential is about 1 ms. An action potential is formed by the interaction of sodium and potassium channels in the cell membrane [Purves et al., 2008]. In the cuneate nucleus high voltage activated calcium channels are also contributing to the generation of an action potential as described below [Spanne, 2011]. The system is stiff, since the fast dynamics are an order of magnitude faster than the rest of the events of the neuron. This together with the fact that the timing of the action potentials are stochastic [Spanne et al., 2014] is the reason that the action potentials are artificially created in this project.

The model of the cuneate neuron

There are some well established mathematical neuron models such as the Rulkov map [Rulkov, 2002], the FitzHugh-Nagumo model [Nagumo et al., 1962; FitzHugh, 1961] and the Hodgkin-Huxley model (Eq. (2.1)) [Hodgkin and Huxley, 1952]. They all have in common that they are approximations of the biophysical processes that take place in the cells.

The model used in this thesis is a conductance-based model. This is the most basic biophysical representation of a neuron. The lipid bilayer of the cell membrane is represented by a capacitor and the ion channels are represented by conductances [Skinner, 2006]. The ion currents in conductance-based models try to individually pull the membrane potential towards its respective reversal potential E. In an electrical context the driving force of the ions acts as a battery. The driving force of an ion is proportional to the difference between the voltage of the membrane potential

and the ion's reversal potential [Purves et al., 2008]. We have that

$$C_m \frac{dV(t)}{dt} = -\sum I_i(t,V), \tag{2.1}$$

where C_m is the capacitance of the cell membrane, $V(t)$ is the membrane potential and I_i is the voltage-dependent ion currents. A circuit diagram of the original Hodgkin-Huxley model can be seen in Fig. 2.1.

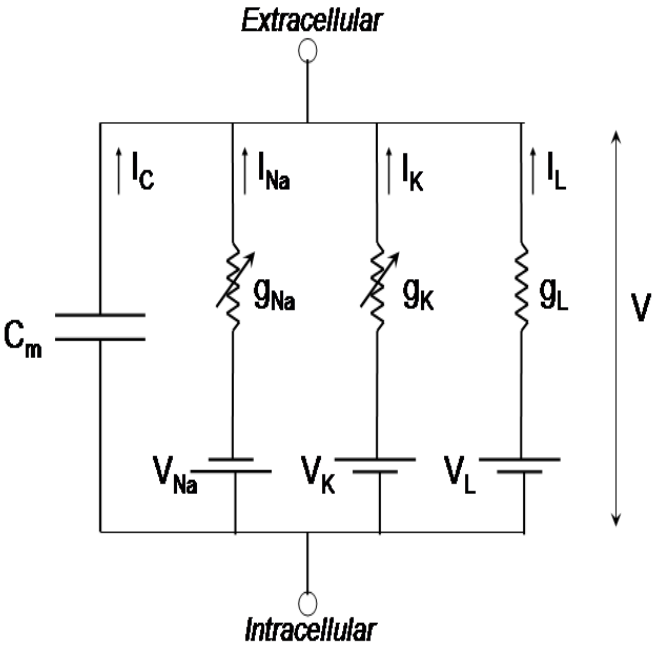

Figure 2.1 A circuit diagram of how the membrane potential is created at the cell membrane. Source: [Skinner, 2006].

Hodgkin and Huxley (1952) proposed a model of the membrane potential of the neuron consisting of several states modeling the activation and inactivation of the sodium and potassium channels that generate the action potentials. An action potential is created by a feedback loop. The rise of the action potential is caused by activation of sodium channels. The rapid decay of the action potential is caused by a combination of inactivation of sodium channels and an activation of potassium channels. Throughout the years the original model by Hodgkin and Huxley

[Hodgkin and Huxley, 1952] has been widely accepted and used. It is often altered by adding ion channels of for example Ca^{2+}. The original model consists of four states, one describing the membrane potential and the other three modeling the activation and inactivation variables. The model of the cuneate neuron used in this thesis is a modified version of the Hodgkin Huxley model.

In addition to the sodium and potassium currents there are dynamics of the neuron that operate with slower time scales. These are the low voltage activated (LVA) calcium channels and the calcium-dependent potassium currents. They are characteristics of the cuneate neuron. These currents of ions flow in or out of the cell for several milliseconds, while the sodium current endure a fraction of a millisecond. These currents accomplish fine tuning of the membrane potential. The cuneate neuron also has Ca^{2+}-dependent potassium currents that cause a strong hyperpolarization of the membrane potential after a burst. Bursting is when the neuron fire groups of action potentials, as can be seen in Fig. 2.5. The potassium channels react to the depolarization of the membrane potential and to the high concentration of Ca^{2+} in the cell [Spanne, 2011]. The calcium dynamics can also be modeled using only high voltage activated (HVA) calcium channels [Saarinen et al., 2008].

The model used in this thesis Eq. (2.2) consists of six states. These states are described in Table 2.1. The parameters of the model are described in Table 2.2. The potassium current is, as stated above, dependent both on the voltage of the membrane potential and the Ca^{2+} concentration at the cell membrane. The conductances act like a weight on the ion currents that determine how big part each of the currents play in creating the potential across the cell membrane. The conductance increases with increasing amount of ion channels in the cell membrane. When the membrane potential is lower than E_i voltage the current becomes positive and vice verse. The parameter D_{Ca} determines how much the calcium current affect the calcium concentration of the cell. The parameter a_i is the membrane potential value (equilibrium potential) that determines when the voltage gated ion channels activate or inactivate. The parameter b_i determines in what range of the membrane potential in the vicinity of a the voltage gated ion channels activate or inactivate. The a_i values are usually approximately the same as the ion's respective reversal potential because that is when the respective ion channels are open. The equation of the activation and inactivation variables consists of a sigmoid subtracted by the activation variable, these sigmoids can be seen in Fig. 2.2 and Fig. 2.3. The time constant τ_i determines how fast or slow the inactivation or activation is, a small τ gives a fast activation or inactivation. The system has a current that is not voltage dependent and that is the leak current, which is caused by the leakage of ions through the cell membrane. This sums up to 24 parameters. The parameter values used in this project were found by Spanne [2011].

$$
\begin{aligned}
\frac{dx_1}{dt} &= \frac{1}{C_m}(-g_L(x_1-E_L)-g_{Ca}x_3^3x_4(x_1-E_{Ca})-g_Kx_5^4x_6^4(x_1-E_K)+I_{app}) \\
\frac{dx_2}{dt} &= D_{Ca}g_{Ca}x_3^3x_4(x_1-E_{Ca})+\frac{([\mathrm{Ca}^{2+}]_{rest}-x_2])}{\tau_{[\mathrm{Ca}^{2+}]}} \\
\frac{dx_3}{dt} &= \frac{1}{\tau_3}\left(\frac{1}{1+e^{\frac{a_3-x_1}{b_3}}}-x_3\right) \\
\frac{dx_4}{dt} &= \frac{1}{\tau_4}\left(1+\frac{-1}{1+e^{\frac{a_4-x_1}{b_4}}}-x_4\right) \\
\frac{dx_5}{dt} &= \frac{1}{\tau_5}\left(\frac{1}{1+e^{\frac{a_5-x_2}{b_5}}}-x_5\right) \\
\frac{dx_6}{dt} &= \frac{1}{\tau_6}\left(\frac{1}{1+e^{\frac{a_6-x_1}{b_6}}}-x_6\right)
\end{aligned}
\tag{2.2}
$$

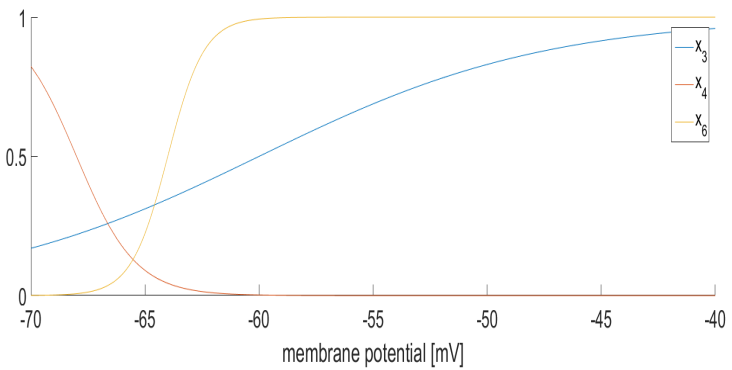

Figure 2.2 The sigmoid functions that describe the equilibrium of the voltage-dependent activation and inactivation variables.

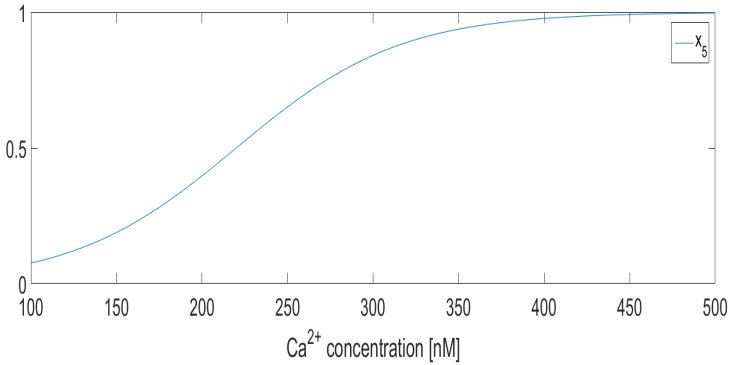

Figure 2.3 The sigmoid functions that describe the equilibrium of the calcium-dependent activation variable of the potassium current.

Table 2.1 The states of the model

x_1	Membrane potential.
x_2	Ca^{2+}-concentration close to the cell membrane.
x_3	Voltage-dependent Ca^{2+} channel activation variable.
x_4	Voltage-dependent Ca^{2+} channel inactivation variable.
x_5	Ca^{2+}-dependent potassium channel activation variable.
x_6	Voltage-dependent potassium channel activation variable.

Table 2.2 The parameters of the model

g_i	Conductance of each ion current.
E_i	Reversal potential of each ion.
I_{app}	Time-dependent function modeling the applied current.
D_{Ca}	Scaling constant of the calcium concentration.
$[Ca^{2+}]_{rest}$	Resting concentration of Ca^{2+} in the cell.
$\tau_{[Ca^{2+}]}$	Time constant of the Ca^{2+}-concentration.
a_i	Center of each sigmoid.
b_i	Slope of each sigmoid.
τ_i	Time constant of the voltage gated ion channels.
C_m	Membrane capacitance.
V_{boost}	Change of membrane potential after a spike.
$[Ca^{2+}]_{boost}$	Change of calcium concentration after a spike.

A big challenge when modeling neurons is the timing of the action potentials, since the initiation is stochastic [Spanne et al., 2014]. Therefore, the model artifi-

cially inserts the spikes at the recorded spike times. After each spike, the membrane potential, x_1, and the calcium concentration, x_2, are reset to new values while the other states are unchanged. The reset mechanism is described in Eq. (2.3).

$$\begin{aligned} x_1(t_{spike}+\Delta t) &= E_L - I_{app}(t_{spike})/g_L + V_{boost} \\ x_2(t_{spike}+\Delta t) &= x_2(t_{spike}) + [Ca^{2+}]_{boost} \end{aligned} \tag{2.3}$$

The parameters V_{boost} and $[Ca^{2+}]_{boost}$ define how much the membrane potential and calcium concentration change after the spikes.

Identifiability and parameter optimization

System identification is an important part of modeling studies. It involves building models by using data. There are different methods to estimate and identify parameter sets for the model at hand [Johansson, 1993]. The identifiability of the parameters of the Hodgkin-Huxley model has not been widely considered [Walch and Eisenberg, 2015]. A study [Walch and Eisenberg, 2015] has shown that some of the parameters of the Hodgkin-Huxley model are identifiable under certain conditions. In this project the amount of data that is needed for identification of parameters have been limited and the focus has not been as much on the identification of parameters as on developing a method to compare a model and a data set. When fitting a model to data it is also important to differentiate between the inability of the model to fit the data due to lack of model complexity and due unaccounted for disturbances [Johansson, 1993].

Parameter optimization of neuronal models is the process of identifying parameters that give a neuron model a desired electrical activity pattern. It is not feasible to find all parameter values of a neuron modelby doing experimental measurments. There are several ways to find good sets of model parameters [Prinz, 2007]. Hand-tuning is one way to find parameters. Hand-tuning is the act of manually changing one or a few parameters at a time until the desired electrical pattern is achieved. An advantage with this method is that a goodness function or an advanced optimization algorithm is not necessary. A downside is that it is subjective and time consuming [Skinner, 2006]. This method was used by for example Nadim and collaborators when building a model of the leech heartbeat elemental oscillator [Nadim et al., 1995]. Another method for parameter optimization is parameter space exploration, such as the Nelder-Mead algorithm [Lagarias et al., 1998], which is being used in this thesis. A benefit with this method is that it provides information about the behavior of the model throughout the parameter space. A disadvantage is that it is computationally expensive [Skinner, 2006]. A third example of a parameter optimization method is evolutionary algorithms. This method was used by for example Taylor and collaborators when they optimized motor neuron synchronization [Taylor and Enoka, 2004]. An advantage with evolutionary algorithms is that they are computationally efficient [Moles et al., 2003], a disadvantage is that the result can be very sensitive to the choice of goodness function [Skinner, 2006].

Examples of existing goodness measure methods

The main purpose of this project is to propose an evaluation method or goodness measure that defines how well a neuron model mimic neuronal recordings. There exist a few already developed and used methods to measure the quality of neuron models. Some examples of such methods are:

- Visual resemblance of the model voltage trace and the recorded voltage trace. This method is simple because it requires no programming skills, a downside is that it is subjective and it can not be used for computerized parameter optimization [Guckenheimer et al., 1993].
- Similarities between the characteristics of the model voltage trace and the recorded trace, for example spike amplitude or inter-spike intervals [Bhalla and Bower, 1993]. To quantify the similarities between the characteristics of the model and the recordings requires algorithms that compute for example the spike amplitude. A benefit of this method is that it is not computationally expensive and it is objective. A downside is that the method is not able to measure the subthreshold dynamics of the model.
- Using the root-mean-square difference between the recorded voltage trace and the model voltage trace [Bhalla and Bower, 1993]. A big problem with this method is that when the spikes in the model are off just a little bit in time it causes a big error. The error does not depend on how far off the spike is, which is an even bigger issue. An advantage with this method is that it is very useful for voltage traces without spikes, where it is an accurate and objective error measurement [Brookings et al., 2014].
- So called all-or-non measures that define goodness based on whether the neuron model pattern is of the same type as the recording, for example tonic firing or bursting [Prinz et al., 2003; Prinz et al., 2004]. A benefit with the all-or-non measure is that it does not require advanced programming skills and computer algorithms. A problem with all or non measurement is that the method is not accurate.

A new evaluation method needs to be developed for situations when the methods mentioned above are insufficient like in the case with the model of the cuneate nucleus.

2.2 The cuneate nucleus

The cuneate nucleus (CN) can be found in the lower brain stem, see Fig. 2.4. Something that is special about the CN is that the information travels directly to the CN from the peripheral skin sensors. The peripheral skin sensors are primary afferents that send signals regarding touch to the brain. According to the so called

”labeled-line-theory”, the CN does not affect the signals that travel through the labeled afferent fibers from the peripheral skin sensors through the CN to the primary somatosensory cortex [Culberson and Brushart, 1989]. However, more recent findings suggest that the CN has a more important role, it preprocesses the information before it reaches the cortex [Jörntell et al., 2014].

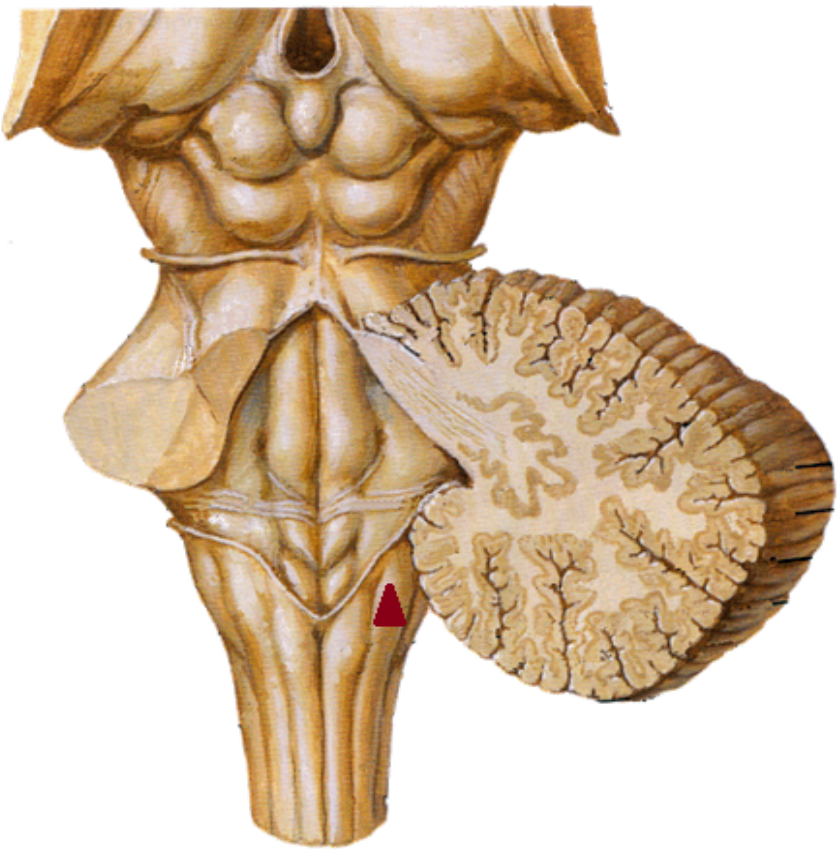

Figure 2.4 The back side of the medulla, which is the lower part of the brainstem. The cuneate nucleus is marked with a red triangle. Source: [Walker, 2013].

One of the characteristics of the CN is the ability of firing doublets or triplets of spikes spontaneously without external input. This can be seen in Fig. 2.5, which shows a recorded trace where the neuron fires spikes at a very high frequency (1000 Hz) [Spanne, 2011].

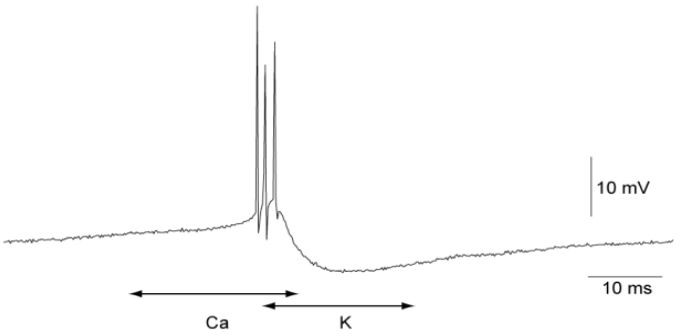

Figure 2.5 A recorded trace that shows the calcium dynamics that contribute to the bursting of the cuneate neuron. Source: [Spanne, 2011].

The cuneate neurons exhibit so called rebound firing, as can be seen in Fig. 2.6. Rebound firing is defined as ”a brief but strong hyper-polarizing input transiently increases their firing rate to much higher levels compared with that prior to the inhibitory input” [Alviña et al., 2009]. The cuneate neurons have many voltage gated calcium channels [Reboreda et al., 2003]. The rebound firing of the cuneate nucleus can be provoked under controlled circumstances as can be seen in Fig. 2.6, which (together with the large amount of calcium channels) shows that this spiking behavior is caused by an intrinsic dynamic such as the one of the voltage gated calcium channels.

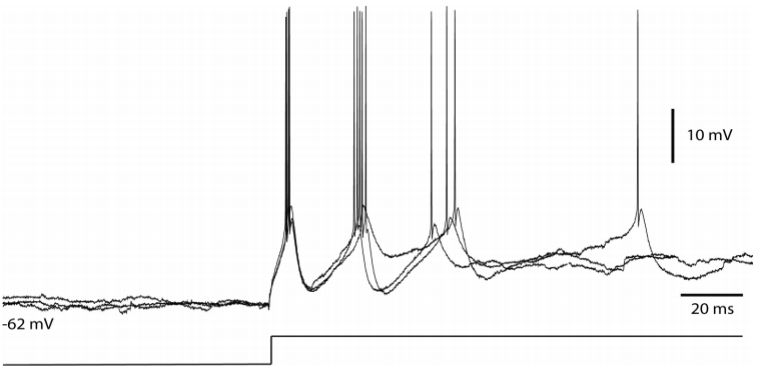

Figure 2.6 Rebound firing in the cuneate nucleus. Source: [Spanne, 2011].

2.3 Sensitivity Analysis

Sensitivity analysis (SA) reveals how changes of the model parameters affect the model output. There are many reasons to perform SA. In this thesis, it is done to investigate what parameters of the model contribute to the output variability, and to find out if there are parameters that are insensitive.

There are two types of SA, global and local. A global sensitivity analysis method (GSA) can be used for non-linear models, like the one in this thesis, or when different input signals are affected by uncertainties. Local methods are often referred to as one-at-a-time (OAT) measures. By using partial derivatives they assess how varying one parameter affects the output while keeping the other parameters at a nominal value. GSA on the other hand evaluate the effect of a parameter while all the other parameters are being varied at the same time, which gives more information about the sensitivity of the parameters [Campolongo et al., 2011].

SA can be divided into two other other categories, variance based SA and screening. Variance bases SA quantifies exactly how much each parameter contributes to the variability of the output, while screening methods provide a ranking of the parameters' sensitivity. The drawback of variance based methods is their time complexity. Screening methods are not as time consuming [Campolongo et al., 2011].

All GSA approaches can be described through three basic steps [Saltelli et al., 2000]:

1. Sampling the input parameters within their variability space.
2. Evaluating the model against the sampled input parameters.
3. Post-processing the input and output samples together to compute the sensitivity measures.

The screening method used in this thesis is one proposed by [Morris, 1991] and later referred by Campologno and co-workers as the Elementary Effects method or EE [Campolongo et al., 2007]. The method varies one parameter at a time while holding the other parameters fixed. The method is categorized as global because it uses different OAT-instances that are estimated and averaged. Each input parameter is associated with its so-called elementary effect. The elementary effect of a parameter defines the ratio between the variation in the output of the model and the variation of the input parameter. The EE method produces two sensitivity measures, μ and σ. The measure μ is the average of many elementary effects and σ is the standard deviation of the same elementary effects.

3

Method

3.1 Model and data choice

To be able to create a general method for measuring the error of a model compared to a data trace recorded from a neuron, the approach taken here has been to start with a simple case and then move on to make the method more general. Once the method works for one neuron type it can be adjusted to work for other neuron types as well.

The cuneate nucleus was chosen as a good example to start with. As described above, it has interesting properties, and there exists a model that captures the special Ca^{2+}-dynamics of the projection neurons [Spanne, 2011]. Another major reason this neuron type was chosen is because it is easy to control the input of the neuron.

The data traces

The data used in this project has been collected by Jörntell and collaborators. For information about the experiments and the data collection see [Jörntell et al., 2014]. The data is recorded from a cat brain *in vivo*. All the experiments were performed according to the ethical regulations and the cats were anesthetized during the experiments. A hyperpolarizing current is injected for 100 ms in the recorded neuron. This controls the membrane potential and keeps it low. When it is released the cell depolarizes and the membrane reaches the threshold for action potential and fires spikes. While injecting the current in the neuron an artifact from the experiment is added to the data trace. This artifact appears because the pipette used in the experiment is clogged with small pieces of cell membrane, which creates an extra resistance. This is compensated for by manually modifying the data traces before they are being compared to the mathematical model.

3.2 Solving the system of equations

The system of differential equations Eq. (2.2) was solved using a built-in ODE solver in Matlab called ode15s. It is a variable-step, variable-order (VSVO) solver

that is based on the numerical differentiation formulas of orders 1 to 5 [Shampine and Reichelt, 1997]. At each step, the solver uses the event-option to see if it has reached the time point of a spike. A maximum step size of 5×10^{-4} is required for the solver to be able to get close enough to the spike times. If the solver has reached the time point of a spike it aborts. The ODE solver is then run again from this time point but the membrane potential and the Ca^{2+}-concentration are set to new values. The different solutions from the runs of the ODE solver are all added up as one solution. The reset mechanisms of the membrane potential and calcium concentration are explained in Chapter 2. A threshold-detection algorithm was written to find the spike-times for the data traces.

To facilitate comparison between the model trace and the data trace, they need to be sampled the same way. Thus, each point in the time vector must correspond to a point in the membrane vector. The ODE solver does not give a solution that is sampled in a eqi-temporal manner, the stiff parts of the model are sampled with a higher frequency. The model trace is therefore interpolated with a linear interpolation.

3.3 The evaluation method

The evaluation method proposed in this project is a weighted L2-norm. It consists of three or four parts that are added together and weighted. To capture the timing of an action potential exactly is very difficult since the mechanisms behind the timing are stochastic [Spanne et al., 2014]. However, it is feasible to model the timing of the rise of the membrane potential before the membrane fires a spike. This is the part of the voltage trace between the green dots in Fig. 3.1. To optimize this part of the model an evaluation method consisting of an overall root-mean-square-error (RMS error) plus an extra term with the RMS error of this time window was created, see Eq. (3.1). The output of the evaluation method is denoted E. The vector $e(t)$ is the difference between the two voltage traces, i.e $e(t) = x_{1_m}(t) - x_{1_d}(t)$.

$$E = \sqrt{\frac{1}{N}\sum_{k=0}^{\infty} e^2(t_k)} + \alpha\sqrt{\frac{1}{N}\sum_{k=t_1}^{t_2} e^2(t_k)} \tag{3.1}$$

This evaluation method Eq. (3.1) was able to measure the error at this specific time window. However, when the evaluation method was used to optimize the whole voltage trace it did not give satisfying results. For example, the model was not able to mimic the recording after the spike. This led to the creation of a new evaluation method. The new evaluation method Eq. (3.2) measures the RMS-error at time windows before and after the spikes.

$$E = \alpha\sqrt{\frac{1}{N}\sum_{k=t_1}^{t_2} e^2(t_k)} + \beta\sqrt{\frac{1}{N}\sum_{k=t_3}^{t_4} e^2(t_k)} + \gamma\sqrt{\frac{1}{N}\sum_{k=t_5}^{t_6} e^2(t_k)} + \delta\sqrt{\frac{1}{N}\sum_{k=t_6}^{t_8} e^2(t_k)} \tag{3.2}$$

An example of the different time windows is shown in Fig. 3.1. The first time window (black) measures the error during the time the cell is stimulated. The calcium-dependent potassium current and the calcium current are activated during this time, which causes a slow oscillation of the cell membrane. How well the model mimic this behavior is measured at this time window. The second time window (green) is the same as in the first evaluation method, it measures how well the model captures the rise of the membrane potential just before the first spike. The third time window (pink) measure how accurately the model mimic the dynamics after the spike when the membrane potential hyperpolarizes. For some instances, the membrane potential oscillates with a very low frequency after the spike last spike, see Fig. 3.1. The error at this slow oscillation is not measured by the evaluation method. If there is a second spike, a fourth time window (yellow) measures how well the model fit to the data after the second spike when the membrane potential hyperpolarizes. There are cases where there is a burst which consists of two spikes and then a third spike, in that case the fourth time window measures the error after the third spike. All weights; α,β,γ,δ are equal to 1.

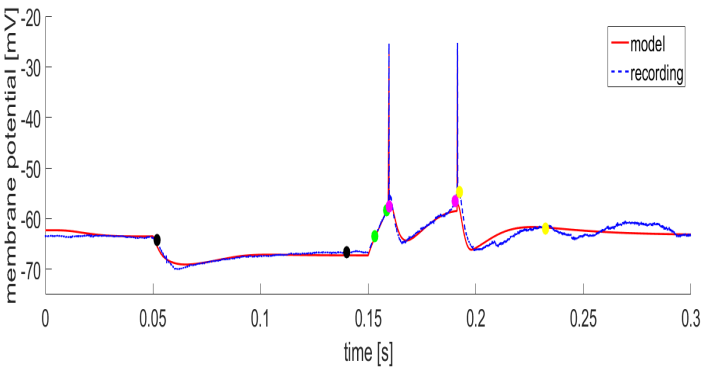

Figure 3.1 An example showing the different time windows where the model is compared to the recorded trace with the L2 norm.

Differential evaluation method

To make sure that the model output mimics the shape of the membrane potential, an attempt was made to compare the first derivative of the model trace and the data

trace. The same time windows as described above where used but the error vector $e(t)$, was defined as in Eq. (3.3).

$$e(t) = \frac{dx_{1_m}(t)}{dt} - \frac{dx_{1_d}(t)}{dt} \tag{3.3}$$

When doing this, the model trace got an offset that was compensated for by subtracting the mean of the difference between the model trace and the recorded trace. Even though the data traces come from good recordings there is inevitably noise, which means that the derivative of the data trace will contain even more noise. Both the model trace and the data trace were filtered with a low-pass filter before the derivative was computed numerically. When the derivative is computed numerically, errors are inevitably introduced in the signal. In this project a first order forward finite difference derivative method was used to compute the derivative. The truncation error for such an algorithm for the derivative is of the order of the step size [Iserles, 2009]. The sample frequency that was used is 50 000 Hz, which gives an error of the order of 10^{-5} at each time point. This size of the error was acceptable since the derivative was on the order of 10^4.

The model evaluation method using the derivative performed equally well at measuring the error of the model as the one using the unprocessed voltage traces.

3.4 Sensitivity analysis

A Matlab toolbox called SAFE [Pianosi et al., 2015] was used to do a sensitivity analysis of the model. The model was analysed with a screening method proposed by Morris [Morris, 1991] called the Elementary Effects method. As stated in Chapter 2, there are three steps in global sensitivity analysis methods (GSA).

Step 1: Sampling the inputs within their variability space. The first step is done by sampling r amount of a vectors and r amount of b vectors (where r is the screening sample size). Both vectors a and b are sets of parameter values for the model, uniformly drawn from the interval $(0.95x_{intial}, 1.05x_{intial})$. The vectors a and b are used to create the vector X, containing r amount of blocks of the size $(M+1 \times M)$, where M is the amount of parameters of the model. The first row in each block consists of the vector a which is the nominal values of that block. The other rows are identical to the first row except for one parameter that is changed in each row of the block, taken from the vector b see Table 3.1.

Table 3.1 Radial scheme, used in the screening method, block of size $(M+1 \times M)$

a_1	a_2	a_3	...	a_k
b_1	a_2	a_3	...	a_k
a_1	b_2	a_3	...	a_k
a_1	a_2	b_3	...	a_k
...				
a_1	a_2	a_3	...	b_k

Step 2: Evaluating the model against the sampled input combinations. An Y vector, consisting of r amount of vectors of size $(M+1)$ is created with the output values from each model evaluation.

Step 3: Post-processing the input/output samples to compute the so called sensitivity measures. The screening method then creates a $(r \times M)$ matrix with the elementary effects of the by iterating diagonally through each block. The elementary effects are described in Eq. (3.4).

$$EE(i,j) = \frac{|Y(k+1) - Y(k_i)|}{|X(k+1,j) - X(k_i,j)|} \cdot Dr(j). \tag{3.4}$$

The index k is the row number of the block in the X matrix and the Y vector respectively, and k_i is the first row in each block. Each elementary effect is normalized by multiplying with $Dr(j)$ where each element in Dr is the range of that parameter. The sensitivity measures μ and σ are then created by averaging and calculating the standard deviation of the columns of the EE matrix respectively.

3.5 Parameter optimization

One of the usages of the the evaluation method is to optimize the parameters of neuron models, which in this thesis is the model of the cuneate nucleus. It is known to be difficult to estimate the parameters of nonlinear systems and it is very hard to use linear systems identification methods to nonlinear systems [Johansson, 1993]. Therefore the heuristic built-in Matlab optimization function fminsearch (which is well suited for nonlinear problems) was used. The function uses the Nelder-Mead algorithm [Lagarias et al., 1998]. The method may find the global minimum but the probability is very small, it is very efficient at finding local minimum compared to other optimization algorithms [Spanne, 2011]. To find a good local minimum, the initial parameters need to be chosen carefully. The model was optimized against several different voltage traces from the same cell with the same stimuli. For the optimization against each data trace, the set of initial parameter values was drawn uniformly from the interval $(0.95X_{\text{nom}}, 1.05X_{\text{nom}})$. The nominal values for the optimization, X_{nom}, are the parameter values Spanne found by hand-tuning the model [Spanne, 2011]. Spanne also used a computational optimization algorithm to enhance the set of parameters but with a different firing mechanism and a different goodness function than the ones used in this project. A much bigger interval was first used, $(0.7X_{\text{nom}}, 1.3X_{\text{nom}})$, but this yielded local minima far from the global. The fminsearch function was at first run for thousands of iterations but a local minimum was found after less than 300 iterations. The optimization function was then run for each trace with a maximum amount of 300 iterations. The new parameter values were then saved and used as initial values for another round of fminsearch with 300 iterations. This does not yield the same results as running the simulation for 600 iterations since the Nelder-Mead algorithm starts out by creating a new simplex by adding 5 % to each parameter value [Lagarias et al., 1998]. The second optimization was done to make sure that the evaluation method could be used when optimizing a model with a small error. The new parameter set was better than the previous one.

4

Results

4.1 Sensitivity analysis

The screening method was run with $r = 1000$, where r is the screening sample size. It had a computation time of 6000 s. The result of the screening is shown in Fig. A.1. The boxes show confidence intervals, they were computed with a bootstrap sample size of 10000. The y-axis is the standard deviation of the elementary effects and the x-axis is the mean of the elementary effects. The y-values show the parameters sensitivity to non-linear effects and to interactions. The x-values show the overall sensitivity. There are three parameters that distinguish themselves and have a much higher sensitivity than the other. Those are a_4, E_L and a_3. The parameter a_i is the membrane potential value that determines when the voltage gated ion channels activate or inactivate. The states x_3 and x_4 are the voltage-dependent activation and inactivation variables respectively. E_L is the reversal potential of the leak current. The parameters V_{boost} and $[Ca^{2+}]_{boost}$ have almost 0 sensitivity.

4.2 Parameter optimization

The evaluation method was used to optimize the model of the CN. All the figures from the parameter optimization can be found in the Appendix. The model was optimized against voltage traces from an experiment with a step current of size 60 pA. The injected current inhibits the cell and the membrane potential hyperpolarizes. All figures show traces of a recording from one single experiment and one single cell. The different responses to the step size are due to the stochastic nature of the neuron. The same nominal parameters are being used for all different voltage traces. This means that the shape of all the different traces with the nominal values are identical until the stimuli is released. The compensation of the offset which is described in chapter three differs between the traces which causes the error of the first time window to be different even though the parameters are the same.

The model parameters are allowed to vary without any boundaries during the optimization. In some of the simulations there are parameters that increase or decrease

significantly compared to their initial values. In the simulations where multiple parameters have changed more than 30 % of its initial value during the optimization, the parameter values can be found in tables where X is the set of parameter values.

One spike

The model parameters were optimized for two different traces that contain one spike. The first trace has a fast rise of the membrane potential before the spike (Fig. A.2) and the second trace has a slowly rising membrane potential before the spike (Fig. A.3). One difference between the two simulations is that the activation variable for the potassium current is fully active during the whole simulation for the simulation with the slowly rising membrane potential (see in Fig. A.3(c)), while in the first simulation the activation variable varies during the simulation (see Fig. A.2(c)). The second simulation has a much higher total error with the set of nominal parameter values than the first simulation (see Tables 4.1 and 4.2), but after optimization they have about the same total error. Another difference between the two simulations can be seen in the plots showing the Ca^{2+}-concentration, where the Ca^{2+}-concentration changes almost continuously in the first simulation (Fig. A.2(e)) while in the second simulation the concentration of Ca^{2+} is almost constant for a long time and then jumps at the time of the spike (Fig. A.3(e)).

Several of the parameters changed significantly when fitting the model to the recording with a slowly rising membrane potential (Fig. A.3). This can be seen in Table 4.3. Several of the time constants increased a lot, which means that those currents endured for a longer time, which is also what is happening (Fig. A.3(d)). A parameter that increases more than 100 % is the membrane capacitance, C_m. The membrane capacitance determines how much the ion currents affect the membrane potential. An increased capacitance means that the membrane reacts slower to the flow of ions across the cell membrane, which is also what is happening (Fig. A.3).

	Window 1	Window 2	Window 3	Window 4	Total
Error for X_{nom}	1.5	2.7	2.6	n/a	6.8
Error for X_{opt}	0.7	0.7	0.7	n/a	2.1
% of error remaining	47 %	26 %	27 %	n/a	31 %

Table 4.1 A comparison of the error for the nominal parameter values and the parameter values of the optimized model for the recording with a spike preceded by a rapidly rising membrane potential, see Fig. A.2.

	Window 1	Window 2	Window 3	Window 4	Total
Error for X_{nom}	1.5	7.4	2.5	n/a	11.4
Error for X_{opt}	0.6	0.7	1.2	n/a	2.5
% of error remaining	40 %	9 %	48 %	n/a	22 %

Table 4.2 A comparison of the error for the nominal parameter values and the parameter values of the optimized model for the recording with a spike preceded by a slowly rising membrane potential, see Fig. A.3.

	g_L	C_m	$[Ca^{2+}]_{boost}$	τ_3	τ_4	τ_5	b_3
X_{nom}	8.1e-9	4.3e-11	8.3e-8	2.7e-4	2.0e-2	1.2e-3	6.3
X_{opt}	11e-9	9.7e-11	13e-8	6e-4	3.7e-2	1.6e-3	9.7
% increase	38 %	130 %	62 %	134 %	87 %	31 %	54 %

(a) The parameters that increased significantly during the optimization.

	E_{Ca}	g_K	τ_6	b_3	a_5	b_6	D
X_{nom}	120	2.0e-8	1.1e-3	1.3	2.2e-7	0.8	250
X_{opt}	82	1.3e-8	0.6e-3	0.9	1.1e-7	0.3	33
% decrease	31 %	34 %	41 %	31 %	49 %	75 %	87 %

(b) The parameters that decreased significantly during the optimization.

Table 4.3 The parameters that increased or decreased more than 30 % when fitting the model to the recording with a spike preceded by a slowly rising membrane potential.

Two spikes

The model parameters were optimized for a trace containing two spikes (Fig. A.4). The optimized model has a much lower error than the model with the nominal parameter values, (the final error is 18 % of the original error). The biggest improvement can be seen at the rise of the membrane potential after the stimuli is released, where only 2 % of the error remain (see Table 4.4). The model trace containing two spikes exhibits discontinuities in the plot of the Ca^{2+}-concentration (Fig. A.4(e)) just like the second simulation with one spike (Fig. A.3(e)).

The Tables 4.5(a) and 4.5(b) show the biggest increase and decrease of some of the parameters respectively. The potassium current is active during both spikes while the calcium current is active mostly during the first spike (Fig. A.4(d)). Two values that stands out are τ_4 and D. The low D-value explain the discontinuities of the Ca^{2+}-concentration, a very low D-value means that the calcium current does

not affect the Ca^{2+}-concentration of the cell. τ_4 is the time constant of the voltage-dependent calcium channel inactivation variable. An increase of this parameter results in a slower inactivation of the calcium channel. This can be seen in Fig. A.4(c).

	Window 1	Window 2	Window 3	Window 4	Total
Error X_{nominal}	0.8	8.5	2.6	2.1	14.0
Error X_{opt}	0.4	0.2	0.6	1.3	2.5
% of error remaining	50 %	2 %	23 %	62 %	18 %

Table 4.4 A comparison of the error for the initial parameter values and the parameter values of the optimized model for the recording with two spikes, see Fig. A.4.

	$[Ca^{2+}]_{rest}$	τ_4	b_5
X_{nominal}	1.0-7	2.0e-2	8e-8
X_{opt}	1.4-7	4.6e-2	6.4e-8
% increase	37 %	130 %	34 %

(a) The parameters that increased significantly during the optimization.

	D
X_{nom}	250
X_{opt}	18
% decrease	93 %

(b) The parameters that decreased significantly during the optimization.

Table 4.5 The parameters that increased or decreased more than 30 % when fitting the model to the recording with two spikes.

A double spike

The model parameters were optimized for a trace containing a burst (Fig. A.5). The optimized model has a much lower error than the nominal model (the final error is 13 % of the original error). The biggest improvement can be seen at the rise of the membrane potential after the stimuli is released where only 2 % of the error remain (see Table 4.6). The potassium current is active during both spikes while the calcium current is active mostly during the first spike (Fig. A.4(d)).

Tables 4.7(a) and 4.7(b) show the biggest increase and decrease of some of the parameters respectively. It is worth noting that these parameters changed by more than 30 % also when the model was fit to the trace with two spikes.

	Window 1	Window 2	Window 3	Window 4	Total
Error X_{nom}	1.3	9.0	2.4	n/a	12.7
Error X_{opt}	0.8	0.2	0.6	n/a	1.6
% of error remaining	62 %	2 %	25 %	n/a	13 %

Table 4.6 A comparison of the error for the nominal parameter values and the parameter values of the optimized model for the recording with a double spike, see Fig. A.5.

	$[Ca^{2+}]_{rest}$	τ_4
X_{nom}	6.3e-3	1.2e-3
X_{opt}	8.8e-3	1.6e-3
% increase	40 %	32 %

(a) The parameters that increased significantly during the optimization.

	D
X_{nom}	250
X_{opt}	152
% decrease	39 %

(b) The parameters that decreased significantly during the optimization.

Table 4.7 The parameters that increased or decreased more than 30 % when fitting the model to the recording with a double spike.

A double spike and a third spike

The model parameters were optimized for a trace containing a burst with a following spikes (Fig. A.6). The optimized model has a lower error than the model with the nominal parameter values. The improvement of the error is big but not as big as in the cases described above. The error at the different time windows are listed in Table 4.8.

	Window 1	Window 2	Window 3	Window 4	Total
Error X_{nom}	1.0	6.5	3.0	1.2	11.7
Error X_{opt}	0.8	0.2	0.7	0.5	2.2
% of error remaining	80 %	3 %	23 %	42 %	19 %

Table 4.8 A comparison of the error for the nominal parameter values and the parameter values of the optimized model for the recording with a double spike and a third spike, see Fig. A.6.

A double spike and a third and a fourth spike

The model parameters were optimized for a trace containing a burst and two following spikes (Fig. A.7). The optimized model has a lower error than the model

with the nominal parameter values. The optimized model is not able to mimic the behavior of the trace after the third spike (Fig. A.7(b)). The error at the different time windows are listed in Table 4.9.

	Window 1	Window 2	Window 3	Window 4	Total
Error X_{nom}	0.9	7.0	3.0	1.6	12.5
Error X_{opt}	0.8	0.2	0.8	0.9	2.7
% of error remaining	90 %	3 %	27 %	56 %	22 %

Table 4.9 A comparison of the error for the nominal parameter values and the parameter values of the optimized model for the recording with a double spike and with a third and a fourth spike, see Fig. A.7.

5

Discussion

5.1 About the results

Sensitivity

The sensitivity analysis showed that a few parameters has a much higher sensitivity than the other. A high sensitivity means that changes of the parameters affect the quality of the model a lot. The parameters with highest sensitivity were a_4, E_l and a_3. The two a-parameters are the membrane potential values that define the center of the sigmoid of the activation and inactivation of the calcium current. E_l is the reversal potential of the leak current. One reason that the parameters a_3 and a_4 are extra sensitive might be that they play an important role in the calcium dynamics and the evaluation method is aiming to measure the calcium dynamics of the model. This indicates that the evaluation method successfully measures how well the model mimic the calcium dynamic of the neuron. The parameter E_L defines the resting potential of the cell membrane, which means that small changes of E_L may have a big effect on the activity of voltage-dependent variables.

A thought we had was to use sensitivity analysis to speed up the process of parameter optimization by eliminating some of the insensitive parameters of the model. We tried this but it turned out that the optimization time was the same and the error was much bigger.

One of the parameters that vary a lot during the optimization of the model for some recordings is D. It is a parameter that is defined by a relationship between a constant and the size of the area of the cell where the Ca^{2+}-ions are. The parameter decides how much the calcium-current contributes to the calcium concentration. One situation where D decreases by more than 90 % is the simulation with two spikes. The plot of the calcium-concentration (Fig. A.4(e)) clearly shows how the calcium current does not affect the calcium concentration in the cell, since D is so small. However, the result of the sensitivity analysis suggested that the parameter D is not sensitive. The low sensitivity of D might be explained by the fact that the sensitivity analysis was performed for a trace where D was not sensitive. This constant, D, is not likely to vary much during an experiment since the size of the

cell is constant. Thus, the results would probably have been different if D would have been constrained to a narrow interval.

The odd voltage trace

The recording with a very slowly rising membrane potential after the stimuli is released (Fig. A.3) differs from the other since all the other traces exhibit a rapidly rising membrane potential after the stimulus is released. This difference is also clear when looking at how much the parameters change during the optimization (Table 4.3). Several variables change more than 50 %. The parameters in the cell of the recording are not likely to change this much in-between two stimuli. Therefore, this odd behaviour of the cell is probably caused by outer factors that can not be controlled during the experiment.

Limitations of the model

Both recordings with one spike (Figs. A.2 and A.3) or a burst (Fig. A.5) exhibit a slow oscillation with a small amplitude after the spikes. The model is not able to fit to the oscillating membrane potential. There are slow dynamics in the model like the oscillatory dynamics during the inhibition but these slow dynamics are apparently not able to also model the oscillation at the end of the voltage trace. The last time window is not covering the whole oscillation, so one reason the model is not able to fit the oscillation might also be that the time window was to narrow. An option would be to add a fifth time window that covers the whole oscillation.

In the case with a burst and two following spikes the model is not able to capture the last spike. The membrane potential of the optimized model is decreasing at the time point when the spike is inserted. If the model would have been able to handle the spike, the membrane potential would have started to depolarize before the spike. This spike could be caused by the slow oscillation mentioned above or some outer input. This might be the explanation why the model is not able to predict the last spike.

The potassium dynamics

The voltage-dependent activation variable of the potassium current is constant for one simulation (Fig. A.3), and the model still captures the dynamics of the recording well. For the other simulations this activation variable is changing mostly when the model is stimulated. Thus, the variable might be contributing to the slow dynamics during the stimulation of the cell. Since the variable is constant during one of the simulations, it could possibly be replaced with a constant. The number of parameters would be reduced by four by doing that. This would make the model simpler and easier to work with.

5.2 Future work

One issue with the recorded data is that it is stochastic in the sense that when the same cell is stimulated with the exact same stimuli it responds in very different ways. Sometimes when the inhibition of the membrane potential is released the neuron fires one spike and sometimes it fires a double-spike and then another spike, or just a double spike. It would be interesting to investigate which components of the neuron contributes the most to these behaviours. This could done by optimizing the model for a set of, for example, 40 different data traces with the exact same applied current and then comparing the parameters to see which parameters change the most. The variance of the parameters could then be compared to the results from the sensitivity analysis. It would be interesting to find out for example if sensitive parameters vary more than the other.

To make the evaluation method proposed in this thesis more useful it needs to investigated whether it can be used for recordings with several different step size amplitudes. A challenge will probably be to find good weights on the different traces to get parameters that are satisfying for all different step sizes. Furthermore it would be interesting to investigate if this method or a modified version could be used for models of other neuron types.

5.3 Conclusions

The aim of this project has been to develop a measurement of the quality of a neuron model of the cuneate nucleus. The use of a weighted L2-norm proved successful, because the developed method enabled parameter optimization of the model. The evaluation method was able to accurately measure how well the model mimic the calcium dynamics of the cuneate nucleus. The sensitivity analysis showed that the calcium dynamics is significant for the quality of the model. This tool will make it easier to build neuron models that capture the responsive properties of the membrane potential in neuronal *in vivo* recordings.

A

Appendix

A.1 Table of all the parameters

Table A.1 All model parameters

Parameters	Unit	Value	What is known
a_3	mV	-60	appr. same as E_L
a_4	mV	-68	appr. same as E_L
a_5	mV	2.2e-07	appr. same as $[Ca2+]_{rest}$
a_6	mV	-64	appr. same as E_L
b_3	mV	6.3	unknown
b_4	mV	1.3	unknown
b_5	mV	4.8e-08	unknown
b_6	mV	0.8	unknown
g_L	S	8.1e-09	found experimentally
g_{Ca}	S	2.1e-08	(1e-7,1e-9)
g_K	S	2.0e-08	(1e-7,1e-9)
E_L	mV	-62	found experimentally
E_{Ca}	mV	1.2e2	(80, 140)
E_K	mV	-1.0e2	(-110,-70)
$[Ca2+]_{rest}$	M	1.0e-07	(1e-6, 1e-8)
$\tau_{[Ca2+]}$	s	6.3e-3	unkown
τ_3	s	2.7e-04	unkown
τ_4	s	2.0e-2	unkown
τ_5	s	1.2e-3	unkown
τ_6	s	1.1e-3	unkown
C_m:	F	4.2e-11	found experimentally
D:	M/SmVs	2.5e2	found experimentally
$[\mathrm{Ca}^{2+}]_{boost}$:	M	8.3e-8	found experimentally
V_{boost}:	mV	6.7	found experimentally

A.2 Figures

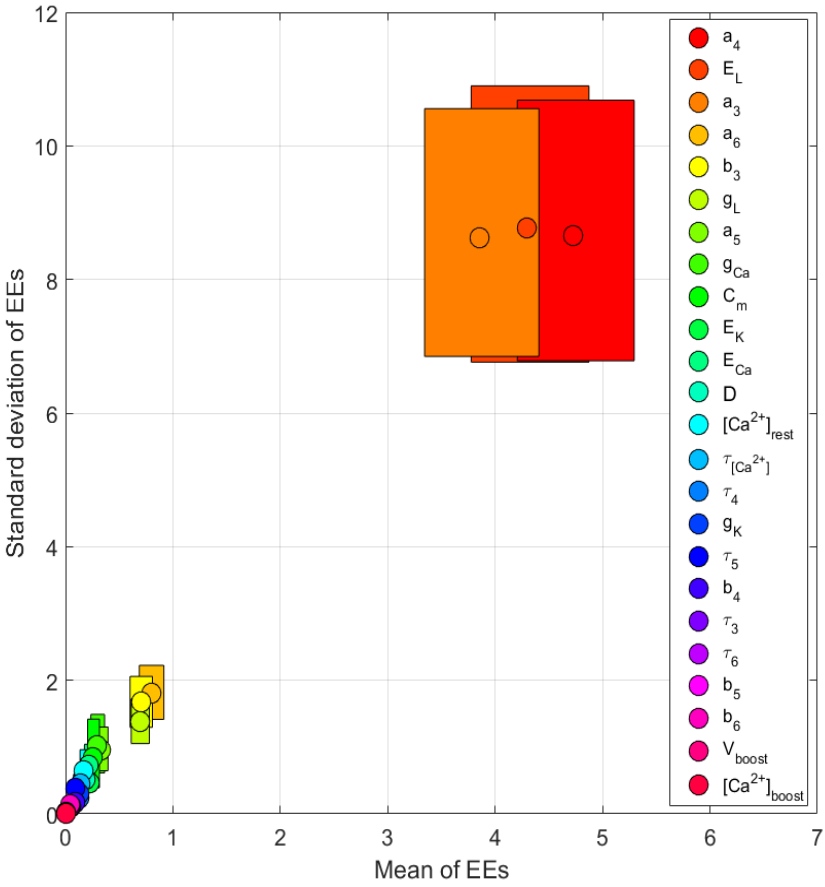

Figure A.1 The result of the sensitivity analysis. The y-axis shows the parameters' sensitivity to interactions and non-linear effects and the x-axis shows the parameters' overall sensitivity. The legend shows the parameters ranked in descending order from top to bottom based on their x-values.

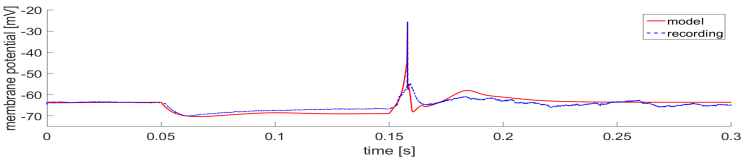

(a) The model with the initial parameters (red) is stimulated with 60 pA for 100 ms beginning at 50 ms. The recorded trace is superimposed (blue).

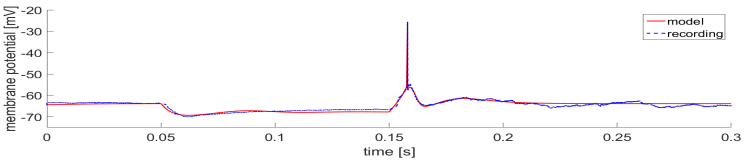

(b) The model with optimized parameters (red) is also stimulated with 60 pA for 100 ms beginning at 50 ms. The recorded trace is superimposed (blue).

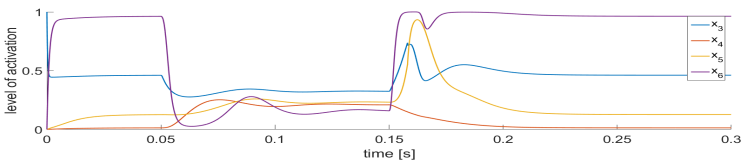

(c) The activation and inactivation variables. The blue and orange curves are the voltage-dependent activation and inactivation variables of the Ca^{2+}-current respectively. The yellow curve is the calcium-dependent activation variable of the potassium current. The purple curve is the voltage-dependent activation variable of the potassium current.

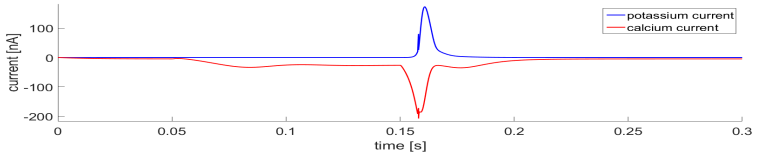

(d) The calcium current (red) and the potassium current (blue).

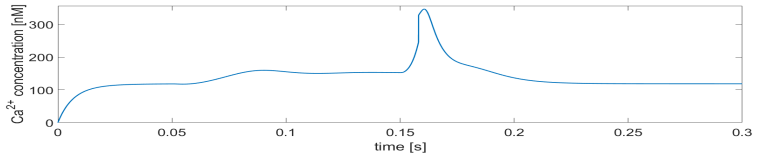

(e) The Ca^{2+}-concentration close to the cell surface changes as a consequence of the Ca^{2+}-current.

Figure A.2 An example where the evaluation method optimizes the parameters of a trace with a spike preceded by a rapidly rising membrane potential.

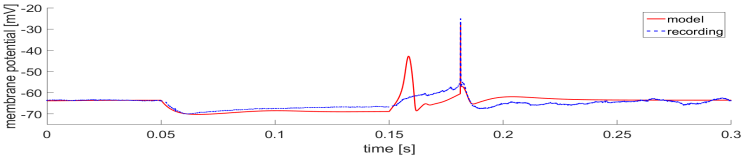

(a) The model with the initial parameters (red) is stimulated with 60 pA for 100 ms beginning at 50 ms. The recorded trace is superimposed (blue).

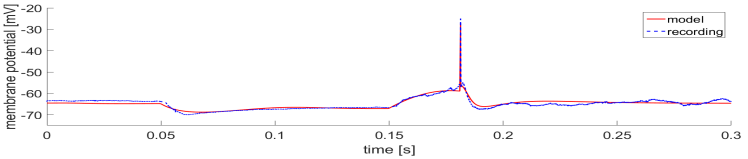

(b) The model with optimized parameters (red) is also stimulated with 60 pA for 100 ms beginning at 50 ms. The recorded trace is superimposed (blue).

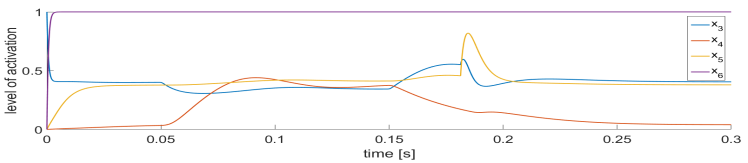

(c) The activation and inactivation variables. The blue and orange curves are the voltage-dependent activation and inactivation variables of the Ca^{2+}-current respectively. The yellow curve is the calcium-dependent activation variable of the potassium current. The purple curve is the voltage-dependent activation variable of the potassium current.

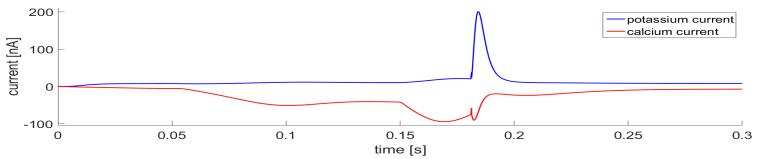

(d) The calcium current (red) and the potassium current (blue).

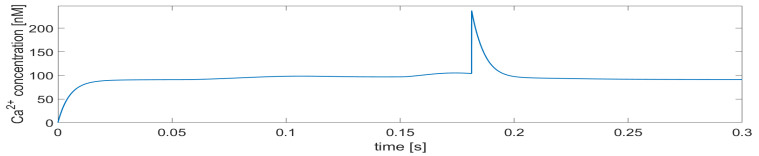

(e) The Ca^{2+}-concentration close to the cell surface changes as a consequence of the Ca^{2+}-current.

Figure A.3 An example where the evaluation method optimizes the parameters of a trace with a spike preceded by a slowly rising membrane potential.

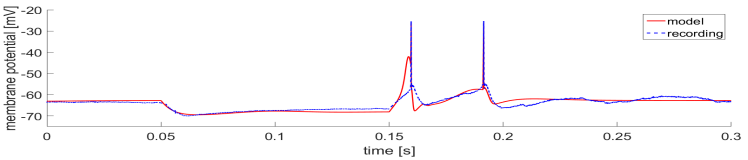

(a) The model with the initial parameters (red) is stimulated with 60 pA for 100 ms beginning at 50 ms. The recorded trace is superimposed (blue).

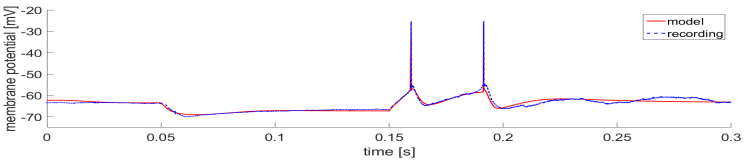

(b) The model with optimized parameters (red) is also stimulated with 60 pA for 100 ms beginning at 50 ms. The recorded trace is superimposed (blue).

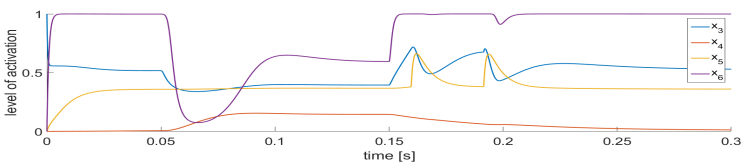

(c) The activation and inactivation variables. The blue and orange curves are the voltage-dependent activation and inactivation variables of the Ca^{2+}-current respectively. The yellow curve is the calcium-dependent activation variable of the potassium current. The purple curve is the voltage-dependent activation variable of the potassium current.

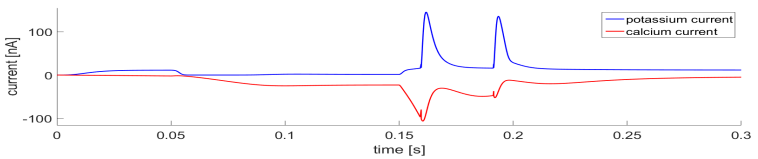

(d) The calcium current (red) and the potassium current (blue).

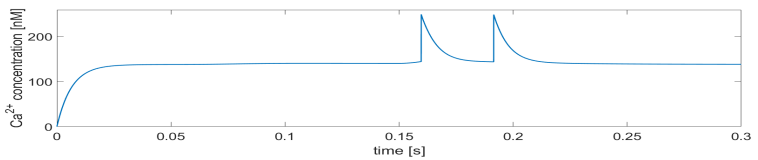

(e) The Ca^{2+}-concentration close to the cell surface changes as a consequence of the Ca^{2+}-current.

Figure A.4 An example where the evaluation method optimizes the parameters of a trace with two spikes.

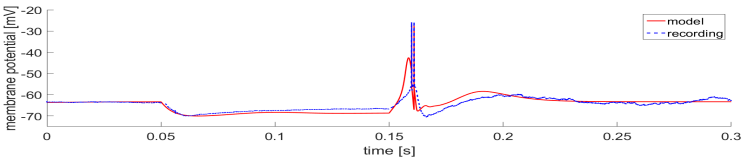

(a) The model with the initial parameters (red) is stimulated with 60 pA for 100 ms beginning at 50 ms. The recorded trace is superimposed (blue).

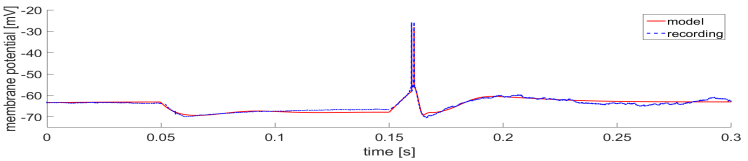

(b) The model with optimized parameters (red) is also stimulated with 60 pA for 100 ms beginning at 50 ms. The recorded trace is superimposed (blue).

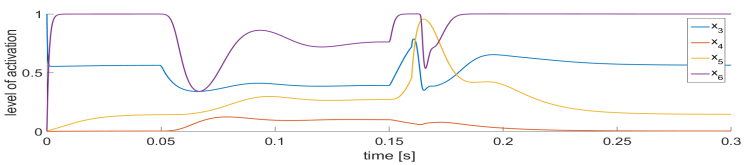

(c) The activation and inactivation variables. The blue and orange curves are the voltage-dependent activation and inactivation variables of the Ca^{2+}-current respectively. The yellow curve is the calcium-dependent activation variable of the potassium current. The purple curve is the voltage-dependent activation variable of the potassium current.

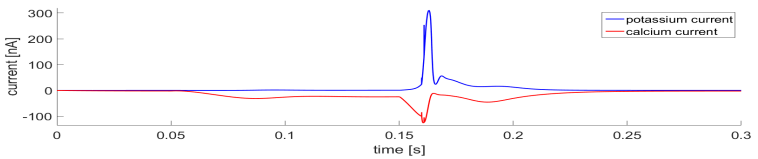

(d) The calcium current (red) and the potassium current (blue).

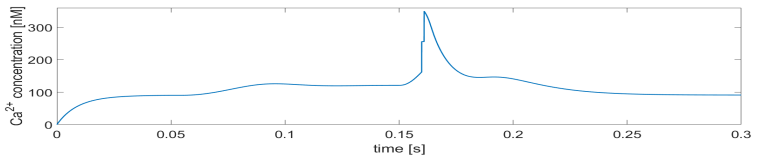

(e) The Ca^{2+}-concentration close to the cell surface changes as a consequence of the Ca^{2+}-current.

Figure A.5 An example where the evaluation method optimizes the parameters of a trace with a double spike.

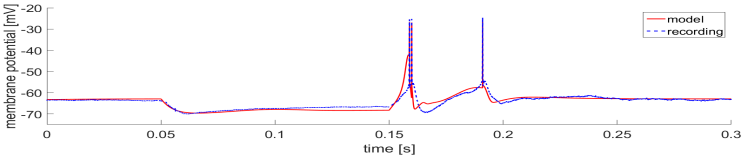

(a) The model with the initial parameters (red) is stimulated with 60 pA for 100 ms beginning at 50 ms. The recorded trace is superimposed (blue).

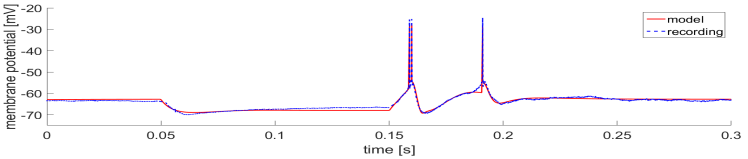

(b) The model with optimized parameters (red) is also stimulated with 60 pA for 100 ms beginning at 50 ms. The recorded trace is superimposed (blue).

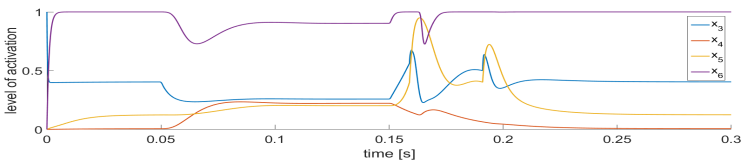

(c) The activation and inactivation variables. The blue and orange curves are the voltage-dependent activation and inactivation variables of the Ca^{2+}-current respectively. The yellow curve is the calcium-dependent activation variable of the potassium current. The purple curve is the voltage-dependent activation variable of the potassium current.

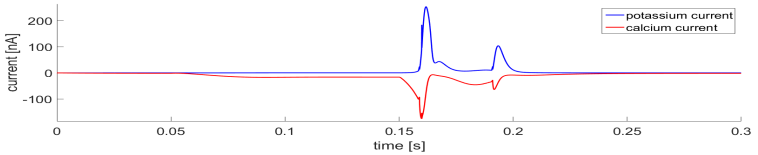

(d) The calcium current (red) and the potassium current (blue).

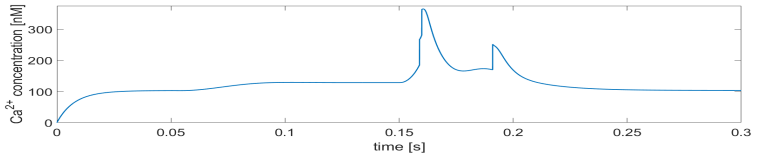

(e) The Ca^{2+}-concentration close to the cell surface changes as a consequence of the Ca^{2+}-current.

Figure A.6 An example where the evaluation method optimizes the parameters of a trace with a double spike and a third spike.

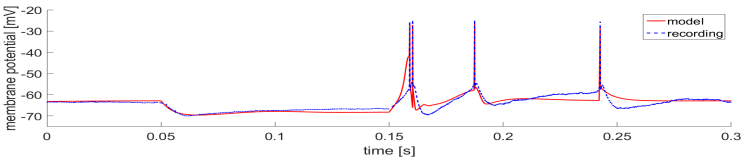

(a) The model with the initial parameters (red) is stimulated with 60 pA for 100 ms beginning at 50 ms. The recorded trace is superimposed (blue).

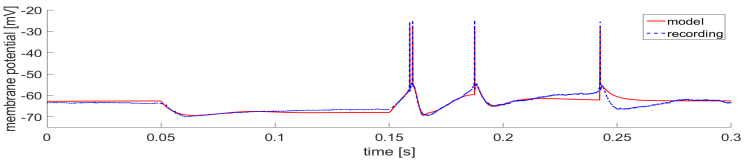

(b) The model with optimized parameters (red) is also stimulated with 60 pA for 100 ms beginning at 50 ms. The recorded trace is superimposed (blue).

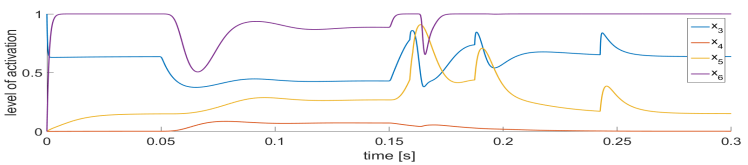

(c) The activation and inactivation variables. The blue and orange curves are the voltage-dependent activation and inactivation variables of the Ca^{2+}-current respectively. The yellow curve is the calcium-dependent activation variable of the potassium current. The purple curve is the voltage-dependent activation variable of the potassium current.

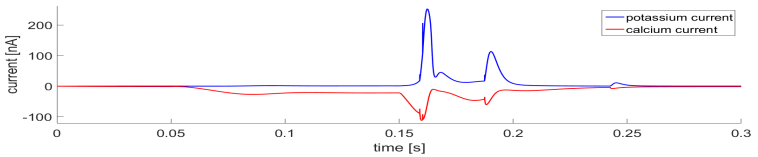

(d) The calcium current (red) and the potassium current (blue).

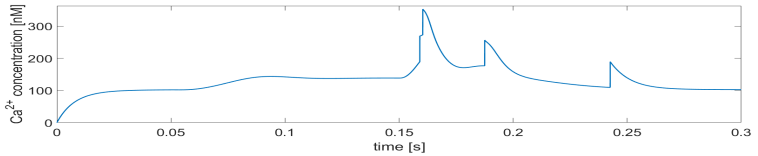

(e) The Ca^{2+}-concentration close to the cell surface changes as a consequence of the Ca^{2+}-current.

Figure A.7 An example where the evaluation method optimizes the parameters of a trace with a double spike and with a third and a fourth spike.

Bibliography

Alviña, K., G. Ellis-Davies, and K. Khodakhah (2009). "T-type calcium channels mediate rebound firing in intact deep cerebellar neurons". *Neuroscience* **158**:2, pp. 635–641.

Bhalla, U. S. and J. M. Bower (1993). "Exploring parameter space in detailed single neuron models: simulations of the mitral and granule cells of the olfactory bulb". *Journal of Neurophysiology* **69**:6, pp. 1948–1965.

Brookings, T., M. L. Goeritz, and E. Marder (2014). "Automatic parameter estimation of multicompartmental neuron models via minimization of trace error with control adjustment". *Journal of Neurophysiology* **112**:9, pp. 2332–2348.

Campolongo, F., J. Cariboni, and A. Saltelli (2007). "An effective screening design for sensitivity analysis of large models". *Environmental Modelling & Software* **22**:10, pp. 1509–1518.

Campolongo, F., A. Saltelli, and J. Cariboni (2011). "From screening to quantitative sensitivity analysis. a unified approach". *Computer Physics Communications* **182**:4, pp. 978–988.

Culberson, J. L. and T. M. Brushart (1989). "Somatotopy of digital nerve projections to the cuneate nucleus in the monkey". *Somatosensory & Motor Research* **6**:3, pp. 319–330.

FitzHugh, R. (1961). "Impulses and physiological states in theoretical models of nerve membrane". *Biophysical Journal* **1**:6, p. 445.

Guckenheimer, J., S. Gueron, and R. M. Harris-Warrick (1993). "Mapping the dynamics of a bursting neuron". *Philosophical Transactions of the Royal Society of London B: Biological Sciences* **341**:1298, pp. 345–359.

Hodgkin, A. L. and A. F. Huxley (1952). "A quantitative description of membrane current and its application to conduction and excitation in nerve". *The Journal of Physiology* **117**:4, p. 500.

Iserles, A. (2009). *A first course in the numerical analysis of differential equations*. 44. Cambridge University Press, Cambridge.

Johansson, R. (1993). *System Modeling and Identification*. Prentice Hall, Englewood Cliffs, New Jersey.

Jörntell, H., F. Bengtsson, P. Geborek, A. Spanne, A. V. Terekhov, and V. Hayward (2014). "Segregation of tactile input features in neurons of the cuneate nucleus". *Neuron* **83**:6, pp. 1444–1452.

Lagarias, J. C., J. A. Reeds, M. H. Wright, and P. E. Wright (1998). "Convergence properties of the nelder–mead simplex method in low dimensions". *SIAM Journal on Optimization* **9**:1, pp. 112–147.

LeMasson, G., E. Marder, and L. Abbott (1993). "Activity-dependent regulation of conductances in model neurons". *Science* **259**, pp. 1915–1915.

Lepora, N. F., P. G. Overton, and K. Gurney (2012). "Efficient fitting of conductance-based model neurons from somatic current clamp". *Journal of Computational Neuroscience* **32**:1, pp. 1–24.

Liu, Z., J. Golowasch, E. Marder, and L. Abbott (1998). "A model neuron with activity-dependent conductances regulated by multiple calcium sensors". *The Journal of Neuroscience* **18**:7, pp. 2309–2320.

Moles, C. G., P. Mendes, and J. R. Banga (2003). "Parameter estimation in biochemical pathways: a comparison of global optimization methods". *Genome Research* **13**:11, pp. 2467–2474.

Morris, M. D. (1991). "Factorial sampling plans for preliminary computational experiments". *Technometrics* **33**:2, pp. 161–174.

Nadim, F., Ø. H. Olsen, E. De Schutter, and R. L. Calabrese (1995). "Modeling the leech heartbeat elemental oscillator i. interactions of intrinsic and synaptic currents". *Journal of Computational Neuroscience* **2**:3, pp. 215–235.

Nagumo, J., S. Arimoto, and S. Yoshizawa (1962). "An active pulse transmission line simulating nerve axon". *Proceedings of the IRE* **50**:10, pp. 2061–2070.

Naundorf, B., F. Wolf, and M. Volgushev (2006). "Unique features of action potential initiation in cortical neurons". *Nature* **440**:7087, pp. 1060–1063.

Pianosi, F., F. Sarrazin, and T. Wagener (2015). "A matlab toolbox for global sensitivity analysis". *Environmental Modelling & Software* **70**, pp. 80–85.

Prinz, A. A. (2007). "Neuronal parameter optimization". *Scholarpedia* **2**:1, p. 1903.

Prinz, A. A., C. P. Billimoria, and E. Marder (2003). "Alternative to hand-tuning conductance-based models: construction and analysis of databases of model neurons". *Journal of Neurophysiology* **90**:6, pp. 3998–4015.

Prinz, A. A., D. Bucher, and E. Marder (2004). "Similar network activity from disparate circuit parameters". *Nature Neuroscience* **7**:12, pp. 1345–1352.

Purves, D., G. Augustine, D Fitzpatrick, W. Hall, A. LaMantia, J. McNamara, and L. White (2008). *Neuroscience, 2008*. Sinauer, Sunderland, Mass.

Reboreda, A., E. Sánchez, M. Romero, and J. A. Lamas (2003). "Intrinsic spontaneous activity and subthreshold oscillations in neurones of the rat dorsal column nuclei in culture". *The Journal of Physiology* **551**:1, pp. 191–205.

Rulkov, N. F. (2002). "Modeling of spiking-bursting neural behavior using two-dimensional map". *Physical Review E* **65**:4, p. 41922.

Saarinen, A., M.-L. Linne, and O. Yli-Harja (2008). "Stochastic differential equation model for cerebellar granule cell excitability". *PLoS Computational Biology* **4**:2, e1000004.

Saltelli, A, K Chan, and E. Scott (2000). *Sensitivity Analysis*. Wiley, Chichester.

Shampine, L. F. and M. W. Reichelt (1997). "The Matlab ODE suite". *SIAM Journal on Scientific Computing* **18**:1, pp. 1–22.

Siegel, M., E. Marder, and L. Abbott (1994). "Activity-dependent current distributions in model neurons". *Proceedings of the National Academy of Sciences* **91**:24, pp. 11308–11312.

Skinner, F. K. (2006). "Conductance-based models". *Scholarpedia* **1**:11, p. 1408.

Spanne, A. (2011). "Developing a model describing the electrophysical behavior of projection neurons in the cuneate nucleus". Unpublished project, Lund University, Lund.

Spanne, A., P. Geborek, F. Bengtsson, and H. Jörntell (2014). "Spike generation estimated from stationary spike trains in a variety of neurons in vivo". *Frontiers in Cellular Neuroscience (in press), doi* **10**.

Taylor, A. L., J.-M. Goaillard, and E. Marder (2009). "How multiple conductances determine electrophysiological properties in a multicompartment model". *The Journal of Neuroscience* **29**:17, pp. 5573–5586.

Taylor, A. M. and R. M. Enoka (2004). "Optimization of input patterns and neuronal properties to evoke motor neuron synchronization". *Journal of Computational Neuroscience* **16**:2, pp. 139–157.

Walch, O. J. and M. C. Eisenberg (2015). "Parameter identifiability and identifiable combinations in generalized hodgkin-huxley models". *arXiv preprint arXiv:1511.05227*.

Walker, W. (2013). *Brain stem. the brain stem consists of midbrain pons medulla oblongata 1 2 3*. URL: `http://slideplayer.com/slide/4637264/#` (visited on 05/10/2016).

Lund University
Department of Automatic Control
Box 118
SE-221 00 Lund Sweden

Document name
MASTER´S THESIS

Date of issue
July 2016

Document Number
ISRN LUTFD2/TFRT--6005--SE

Author(s)
Oscar Flodin

Supervisor
Henrik Jörntell, Neural Basis of Sensorimotor Control, Lund University, Sweden
Carolina Lidström, Dept. of Automatic Control, Lund University, Sweden
Anton Spanne, Neural Basis of Sensorimotor Control, Lund University, Sweden
Kristian Soltesz, Dept. of Automatic Control, Lund University, Sweden
Rolf Johansson, Dept. of Automatic Control, Lund University, Sweden (examiner)

Sponsoring organization

Title and subtitle
Method to measure the quality of a neuron model compared to recorded data

Abstract

In this thesis, a method for evaluating the accuracy of mathematical neuron models is developed, with the objective to both improve the quality and the speed of parameter optimization. To evaluate the method, we used a conductance based model of the cuneate nucleus. The model behavior was evaluated against neurons recorded in vivo. A big challenge when modeling neurons is the timing of the action potentials, since the initiation is stochastic. Therefore, the model artificially inserts the spikes at the recorded spike times. The accuracy of the model is evaluated as its capacity to capture the time evolution of the membrane potential both following and preceding the spikes. The evaluation method uses the L2-norm when comparing a few important time windows of the recording and the model. The method was used to optimize the parameters of the model. Sensitivity analysis is used to learn which model parameters affect the model accuracy the most. The results from the optimization showed that the developed method well describes the quality of the neuron model for different parameters. This tool will make it easier to build models that capture the responsive properties of the membrane potential in neuronal in vivo recordings.

Keywords

Classification system and/or index terms (if any)

Supplementary bibliographical information

ISSN and key title
0280-5316

ISBN

Language
English

Number of pages
1-48

Recipient's notes

Security classification